



ATLAS NOTE

ATLAS-CONF-2012-004

February 14, 2012



Search for gluinos in events with two same-sign leptons, jets and missing transverse momentum with the ATLAS detector in pp collisions at $\sqrt{s} = 7 \text{ TeV}$

The ATLAS Collaboration

1 Introduction

Supersymmetry (SUSY) [1–7] is a theory beyond the Standard Model (SM) which predicts new bosonic partners for the existing fermions and fermionic partners for the known bosons. It may naturally resolve the hierarchy problem [8–11] and unify the fundamental forces of nature [12–15]. In the framework of a generic R -parity conserving minimal supersymmetric extension of the SM (MSSM), SUSY particles are produced in pairs [16, 17] and the lightest supersymmetric particle is stable, providing a possible candidate for dark matter.

The gluino is a strongly-interacting Majorana fermion. Pair-produced gluinos have therefore equal probabilities of producing a pair of leptons that have the same charge (same-sign, SS) and the opposite charge from their decays. The supersymmetric partner of the top quark has two mass eigenstates with \tilde{t}_1 being the lightest. Top quarks and \tilde{t}_1 squarks can be produced in the decay of the gluino via $\tilde{g}\tilde{g} \rightarrow t\bar{t}\tilde{t}_1\tilde{t}_1^*, t\bar{t}\tilde{t}_1^*\tilde{t}_1^*, \bar{t}\bar{t}\tilde{t}_1\tilde{t}_1$ [18–22]. The \tilde{t}_1 squark can further decay to either $b\tilde{\chi}_1^\pm$ or $t\tilde{\chi}_1^0$ producing isolated leptons via the semi-leptonic decay of the top quark or via the leptonic decay of the chargino and thus enriches the signal events with two or more leptons, jets and missing transverse momentum (E_T^{miss}). This analysis considers events with a pair of isolated SS leptons, multiple high- p_T jets and large E_T^{miss} . The requirement of SS leptons in the event suppresses the contribution of SM processes and thus enhances the potential signal significance. Previous ATLAS analysis searching for supersymmetric particle with SS dileptons [23, 24] were not optimized for gluino mediated stop production, which has been studied in the past using only a signature based on 1 lepton plus b -jets [25, 26].

2 The ATLAS Detector

The ATLAS detector [27] consists of inner tracking devices surrounded by a superconducting solenoid, electromagnetic and hadronic calorimeters and a muon spectrometer with a toroidal magnetic field. The inner detector provides precision tracking of charged particles for $|\eta| < 2.5$ [28]. The calorimeter system covers the pseudorapidity range $|\eta| < 4.9$. It is composed of sampling calorimeters with either liquid argon (LAr) or scintillating tiles as the active media. The muon spectrometer provides muon identification and measurement for $|\eta| < 2.7$.

3 Object and Event Selection

Description of the ATLAS detector can be found in Ref. [27]. This search uses pp collision data recorded from March to August 2011 at a center-of-mass energy of 7 TeV. The data set corresponds to a total integrated luminosity of $2.05 \pm 0.08 \text{ fb}^{-1}$ [29, 30] after the application of beam, detector and data quality requirements. Events are selected using single lepton and dilepton triggers that have constant efficiency as a function of lepton p_T above the offline p_T cuts used in the analysis.

Jets are reconstructed from three-dimensional calorimeter energy clusters by using the anti- k_t jet algorithm [31, 32] with a radius parameter of 0.4. The measured jet energy is corrected for inhomogeneities and for the non-compensating nature of the calorimeter by using p_T - and η -dependent correction factors [33]. Only jet candidates with $p_T > 20 \text{ GeV}$ within $|\eta| < 2.8$ are retained. Events with any jet that fails the jet quality criteria designed to remove noise and non-collision backgrounds [33] are rejected.

Electron candidates are required to have $p_T > 10 \text{ GeV}$, $|\eta| < 2.47$ and satisfy the ‘medium’ selection criteria defined in Ref. [34]. Muon candidates are required to have $p_T > 10 \text{ GeV}$, $|\eta| < 2.4$ and are identified by matching an extrapolated inner detector track and one or more track segments in the muon spectrometer [35]. To avoid overlaps, any jet within a distance of $\Delta R = \sqrt{(\Delta\eta)^2 + (\Delta\phi)^2} < 0.2$ from a ‘medium’ electron candidate is discarded. Electron or muon candidates within $\Delta R < 0.4$ of any remaining jet are also discarded.

The calculation of E_T^{miss} [36] is based on the vectorial sum of the p_T of the reconstructed jets (with $p_T > 20$ GeV and $|\eta| < 4.5$), leptons and the calorimeter energy clusters not belonging to reconstructed objects.

During part of the data-taking period, a localized electronics failure in the electromagnetic barrel calorimeter created a dead region in the second and third calorimeter layers ($\Delta\eta \times \Delta\phi \simeq 1.4 \times 0.2$) in which on average 30% of the incident jet energy is not measured. For jets in this region, a correction to their energy is made using the energy depositions in the cells neighbouring the dead region, and this is also propagated to E_T^{miss} . Similarly to what was done in Ref. [37], if this correction projected over the direction of the E_T^{miss} is larger than 10 GeV or 10% of the E_T^{miss} , the event is discarded. Events with reconstructed electrons in the LAr calorimeter dead region are also rejected.

Events in which the two leading leptons ($\ell = e, \mu$) have the same charge are selected. In addition to the baseline object selection described above, electron candidates must pass the ‘tight’ selection criteria in Ref. [34] and be isolated — the scalar sum of p_T of tracks within a cone in the $\eta - \phi$ plane of radius $\Delta R = 0.2$ around the candidate excluding its own track, Σ_{p_T} , must be less than 10% of the electron p_T . Muons must have longitudinal and transverse impact parameter within 1 mm and 0.2 mm of the primary vertex [38], respectively, and $\Sigma_{p_T} < 1.8$ GeV. Events should contain at least two leptons passing the selections described above and with $p_T > 20$ GeV. Only events with at least four jets with $p_T > 50$ GeV are selected.

Furthermore, two separate signal regions are considered: SR1, which requires a cut on $E_T^{\text{miss}} > 150$ GeV; and SR2, which in addition to the E_T^{miss} cut on SR1 also requires a cut on $m_T > 100$ GeV, where m_T is the transverse mass of the E_T^{miss} and the leading lepton defined as $m_T^2 = 2 \cdot p_T^\ell \cdot E_T^{\text{miss}} \cdot (1 - \cos(\Delta\phi(\ell, E_T^{\text{miss}})))$. The signal regions are optimized based on several models where SS dileptons are produced in gluino decays. In signals such as the MSUGRA/CMSSM (minimal supergravity or constrained minimal supersymmetric standard model) [39, 40], the directions of the lepton and $\tilde{\chi}_1^0$ are strongly correlated as they originate from the decay of a common parent particle (usually $\tilde{\chi}_1^\pm$ or $\tilde{\chi}_2^0$). This leads to a softer m_T spectrum than that found in gluino-mediated stop signal models, where the lepton and $\tilde{\chi}_1^0$ originate from different parent particles and are thus uncorrelated.

4 Simulation

Simulated Monte Carlo (MC) event samples are used to aid in the description of the background and to model the SUSY signal. Top-quark pair and single-top production are simulated with MC@NLO [41], fixing the top-quark mass at 172.5 GeV, and using the next-to-leading-order (NLO) parton density function (PDF) set CTEQ6.6 [42]. Samples of W +jets and Z +jets with both light and heavy flavor jets are generated with ALPGEN [43] and PDF set CTEQ6L1 [44]. The fragmentation and hadronization for the ALPGEN and MC@NLO samples are performed with HERWIG [45], using JIMMY [46] for the underlying event. Samples of $t\bar{t}Z$, $t\bar{t}W$ and $t\bar{t}WW$ (referred to as $t\bar{t} + X$) are generated with MADGRAPH [47] interfaced to PYTHIA [48] and normalized to NLO cross sections using a K -factor of 1.3 ± 0.65 [49, 50]. Diboson ($W^\pm W^\mp$, WZ , ZZ) samples are generated with HERWIG and $W^\pm W^\pm qq$ samples are generated with MADGRAPH. SUSY signal processes are simulated for various models using HERWIG++ [45] v2.4.2. The SUSY sample yields are normalized to the results of NLO calculations, as obtained using PROSPINO [51] v2.1. The CTEQ6.6M [52] parameterization of the PDFs is used. The tunings of the MC parameters of Ref. [53] are used in the production of the MC samples, which are processed through a detector simulation [54] based on GEANT4 [55]. Effects of multiple proton-proton interactions per bunch crossing are included in the simulation.

5 Background Estimation

The SM backgrounds are evaluated using a combination of MC simulation and data-driven techniques. SM processes that generate events containing jets which are misidentified as leptons or where a lepton from a b- or c- hadron decay is selected are collectively referred to as “fake-lepton” background which generally consists of semi-leptonic $t\bar{t}$, single top, $W+jets$ and QCD light and heavy-flavour jet production. The contribution from the “fake-lepton” background is estimated from data using a method similar to that described in Ref. [56, 57]. This method defines a loose lepton selection and counts the numbers of observed events containing loose-loose, loose-tight, tight-loose and tight-tight lepton pairs. The probability of loose real leptons to pass the tight selection criteria is obtained using a $Z \rightarrow \ell^+ \ell^-$ sample. The probability of loose fake leptons to pass the tight selection criteria is determined using multijet control samples obtained by requiring two same-sign leptons and low E_T^{miss} . Using these probabilities, relations are obtained for the observed event counts in the signal regions as functions of the numbers of events containing fake-fake, fake-real, real-fake and real-real lepton pairs. These can be solved simultaneously to estimate the number of background events [56, 57]. The results of the estimations have been validated with data in control regions obtained by reversing the E_T^{miss} or jet multiplicity cuts used in the signal regions.

Background events from charge misidentification (electrons which have undergone hard bremsstrahlung with subsequent photon conversion) are estimated using a partially data-driven technique [24]. The probability of charge misidentification is calculated from MC and corrected by consideration of the number of events with SS lepton pairs inside the Z boson mass peak. This probability is applied to $t\bar{t}$ MC events producing $e^\pm \ell^\mp$ pairs to evaluate the number of same-sign events from incorrect charge assignment in each signal region. The probability of misidentifying the charge of a muon and the contributions in the signal regions from charge misidentification of Z/γ^*+jets and other SM backgrounds are negligible.

Contributions from other SM background sources (diboson and $t\bar{t} + X$ processes) are evaluated using the MC samples described above. In these processes, real SS lepton pairs are produced and their contribution to the signal regions can be described reliably with MC. In particular, the contribution from the experimentally unmeasured $t\bar{t} + X$ processed has been studied using several MC generators.

The background from cosmic rays is evaluated with data using the method in Ref. [24] and its contribution is negligible in the signal regions.

6 Systematic Uncertainties

Systematic uncertainties are estimated in the signal regions for the background and for the SUSY signal processes. The primary sources of systematic uncertainties are the jet energy scale calibration, the jet energy resolution, MC modeling uncertainties, uncertainties on object reconstruction and identification, and theoretical cross section uncertainties. In particular, the theory uncertainties on the cross section of the $t\bar{t}+X$ processes are found to be 55% by varying factorization and renormalization scales and 25% due to PDF uncertainties. In addition, 50% uncertainty is assigned on the K -factor used to obtain the NLO cross section for these processes [49]. In the fake-lepton background estimation, systematic uncertainties are assigned to the probabilities of loose fake leptons to pass the tight selection to account for potential different composition of signal and control regions. These uncertainties vary in the 10%-80% range depending on the lepton p_T . The absolute uncertainty for each background source is given in Table 1. Systematic uncertainties on the signal expectations are evaluated through variations of the factorization and renormalization scales in PROSPINO between half and twice their default values, and by including the uncertainty on α_s and on the PDF provided by CTEQ6. Uncertainties are calculated for individual SUSY processes. The total uncertainty varies in the 20%-40% range for the considered MC signal. The systematic uncertainties in signal and backgrounds are correlated when appropriate.

7 Results and Interpretation

Table 1: Number of expected SM background events together with the number of observed events in data. Limits at 95% C.L. on $\sigma_{\text{vis}} = \sigma \times \epsilon \times A$ are also shown. The errors are a combination of the uncertainties due to MC statistics, statistical uncertainties in control regions and systematic uncertainties.

	SR1	SR2
$t\bar{t} + X$	0.37 ± 0.26	0.21 ± 0.16
Diboson	0.05 ± 0.02	0.02 ± 0.01
Fake-lepton	0.34 ± 0.20	< 0.17
Charge mis-ID	0.08 ± 0.01	0.039 ± 0.007
Total SM	0.84 ± 0.33	0.27 ± 0.24
Observed	0	0
σ_{vis}	$< 1.6 \text{ fb}$	$< 1.5 \text{ fb}$

Figure 1 shows the distribution for the number of jets with $p_T > 50 \text{ GeV}$ for events with 2 SS leptons and the E_T^{miss} distribution for events with 2 SS leptons and at least four jets with $p_T > 50 \text{ GeV}$. The contributions from all the SM backgrounds are shown together with their statistical and systematic uncertainties. For illustration, the distribution for a signal obtained with the decay $\tilde{g} \rightarrow t\bar{t}\tilde{\chi}_1^0$ in $\tilde{g}\tilde{g}$ pair-produced events with $m_{\tilde{g}} = 650 \text{ GeV}$ and $m_{\tilde{\chi}_1^0} = 150 \text{ GeV}$ is also shown. The data are in agreement with the SM background expectation and once four jets of $p_T > 50 \text{ GeV}$ are required no event is observed with $E_T^{\text{miss}} > 150 \text{ GeV}$.

Table 1 shows the number of expected events in the signal regions for each background source together with the observed number of events. In SR1 the dominant backgrounds are $t\bar{t} + X$ and fake leptons while in SR2 $t\bar{t} + X$ is the main background. The contribution from the SM is estimated to be less than one event for each signal region with no events observed in data. Therefore, limits at 95% confidence level (C.L.) are derived on $\sigma_{\text{vis}} = \sigma \times \epsilon \times A$ where σ is the total production cross sections for any new signal producing SS dileptons, A is the acceptance defined by fraction of events passing geometric and kinematic cuts at particle level and ϵ is the detector reconstruction, identification and trigger efficiency. Limits are set using the CLs prescription, as described in Ref. [58]. The results are given in Table 1 for each signal region.

The results obtained in SR2 are interpreted in a simplified model where only gluinos are produced in pairs, the stop ($m_{\tilde{t}} = 1.2 \text{ TeV}$) is heavier than the gluino, and only the gluino three-body decay via an off-shell stop ($\tilde{g} \rightarrow t\bar{t}\tilde{\chi}_1^0$) is allowed. Figure 2 shows the limit in the gluino-neutralino mass plane. Gluino masses below 650 (720) GeV for neutralino masses below 215 (100) GeV are excluded at 95% confidence level. The results can be generalised in terms of 95% C.L. upper cross section limits for $\tilde{g}\tilde{g}$ pair production processes with the produced particles decaying into $t\bar{t}\tilde{\chi}_1^0$ final states, as also shown in Figure 2.

The results in SR2 are also interpreted in the MSSM 24-parameter framework as defined in [59] considering gluino pair production followed by the $\tilde{g} \rightarrow \tilde{t}_1 t$ decay. Only stop decays via $\tilde{t}_1 \rightarrow b\tilde{\chi}_1^\pm$ are considered. All other squark as well as slepton masses are larger than 1 TeV and $m_{\tilde{\chi}_1^\pm} = 2m_{\tilde{\chi}_1^0}$ with a neutralino mass of 60 GeV. Figure 3 shows the exclusion limit as a function of gluino and stop masses, where gluino masses below 670 GeV are excluded for stop masses below 460 GeV.

The results in SR1 are interpreted within the MSUGRA-CMSSM framework in terms of limits on the universal scalar and gaugino mass parameters m_0 and $m_{1/2}$, as shown in Figure 4. These are presented for fixed values of the universal trilinear coupling parameter $A_0 = 0$, ratio of the vacuum expectation values of the two Higgs doublets $\tan\beta = 10$, and Higgs mixing parameter $\mu > 0$. In this model, values of

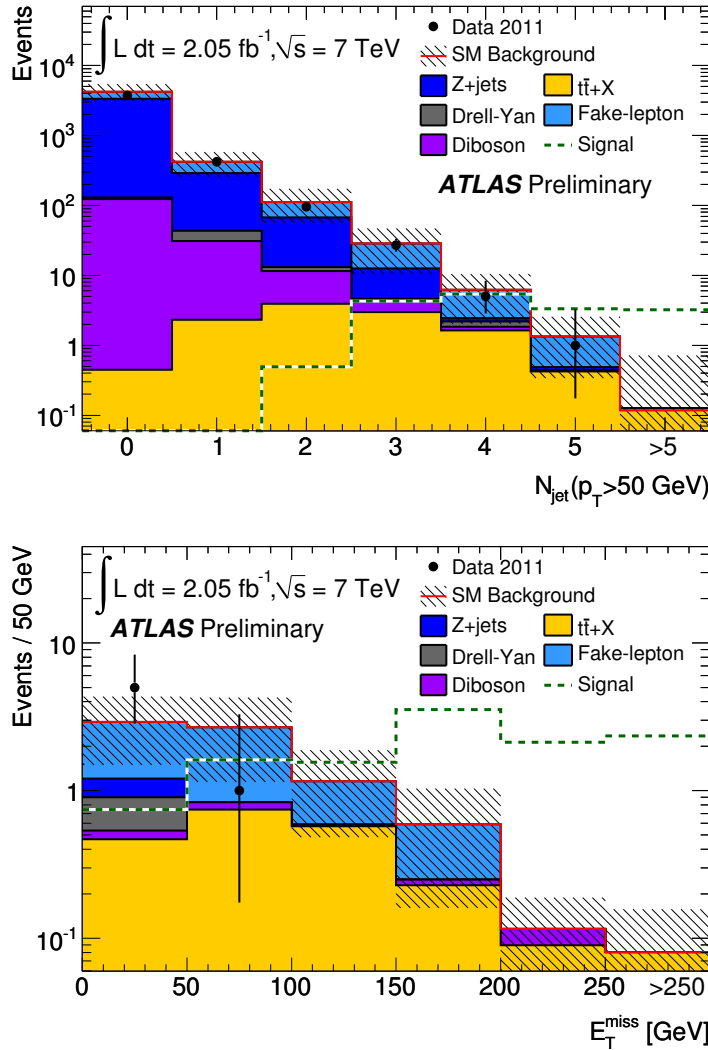


Figure 1: Number of jets with $p_T > 50$ GeV for events with 2 same-sign leptons (top) and the E_T^{miss} distribution for events with 2 same-sign leptons and at least 4 jets with $p_T > 50$ GeV (bottom). Errors on data points are statistical, while the error band on the SM background represents the total uncertainty. The component labelled “Fake leptons” is evaluated using data as described in the text. The components labelled “Z+jets” and “Drell-Yan” are from MC. No estimation of the charge mis-ID is included in the distribution. The component labelled “Signal” corresponds to a signal obtained with the decay $\tilde{g} \rightarrow t\bar{t}\tilde{\chi}_1^0$ via off mass-shell \tilde{t} ($m_{\tilde{t}} = 1.2$ TeV) in $\tilde{g}\tilde{g}$ pair-produced events with $m_{\tilde{g}} = 650$ GeV and $m_{\tilde{\chi}_1^0} = 150$ GeV.

$m_{1/2}$ below 310 (180) GeV are excluded for m_0 values below 750 GeV (above 2 TeV). This is equivalent to the exclusion of gluino masses below ~ 550 GeV independently of the squark mass and gluino masses below 750 GeV for squark masses below 1 TeV.

8 Conclusions

In summary, a search for SUSY with two same-sign leptons, jets and missing transverse momentum has been performed using 2.05 fb^{-1} of ATLAS data. With no events observed in the selected signal

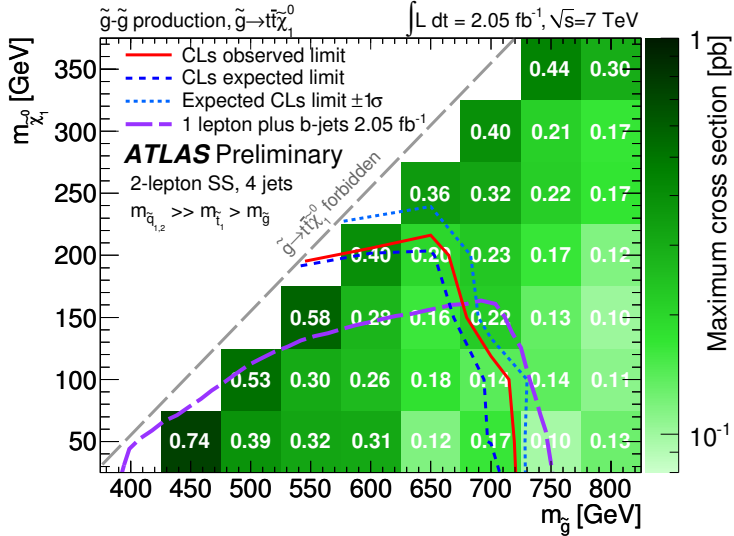


Figure 2: Expected and observed 95% C.L. exclusion limits in the $\tilde{g} \rightarrow t\bar{t}\tilde{\chi}_1^0$ (via off mass-shell \tilde{t} , $m_{\tilde{t}} = 1.2$ TeV) simplified model as a function of the gluino and neutralino masses, together with existing limits [26]. The lower part of the $\pm 1\sigma$ band lies outside the range of the figure. The upper production cross section limits at 95% C.L. are also shown.

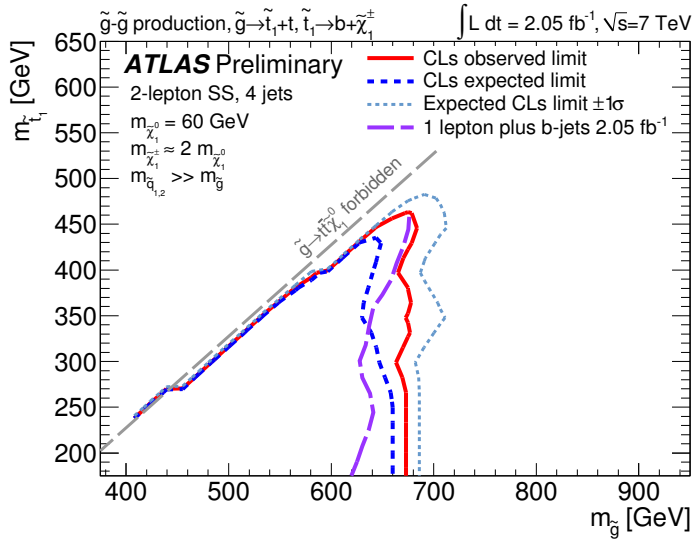


Figure 3: Expected and observed 95% C.L. exclusion limits in the phenomenological MSSM as a function of the gluino and stop masses assuming that $m_{\tilde{\chi}_1^\pm} = 2m_{\tilde{\chi}_1^0}$. The lower part of the $\pm 1\sigma$ band lies outside the range of the figure.

regions, limits have been derived in the context of simplified models where top quarks are produced in gluino decays and MSUGRA/CMSSM scenarios. In all these signal models, gluino masses below 550 GeV are excluded within the parameter space considered and gluino masses up to 700-750 GeV can be excluded depending on the model parameters. The results of this analysis are comparable to other ATLAS searches [26, 64, 65] and in some cases they extend the current exclusion limits on the gluino

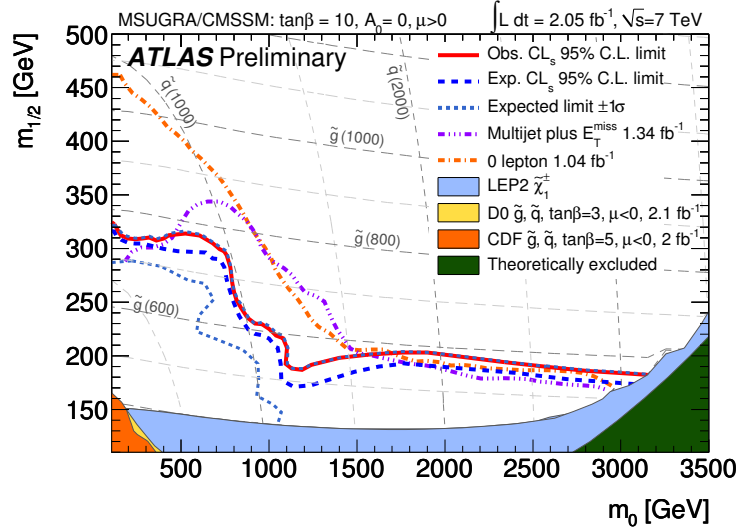


Figure 4: Expected and observed 95% C.L. exclusion limits in the MSUGRA/CMSSM ($m_0, m_{1/2}$) plane for $\tan\beta = 10, A_0 = 0$ and $\mu > 0$, together with existing limits [60–65].

mass.

References

- [1] P. Ramond, *Dual Theory for Free Fermions*, Phys. Rev. **D3** (1971) 2415–2418.
- [2] Y. Golfand and E. Likhtman, *Extension of the Algebra of Poincare Group Generators and Violation of p Invariance*, JETP Lett. **13** (1971) 323–326.
- [3] A. Neveu and J. H. Schwarz, *Factorizable dual model of pions*, Nucl. Phys. **B31** (1971) 86–112.
- [4] A. Neveu and J. H. Schwarz, *Quark Model of Dual Pions*, Phys. Rev. **D4** (1971) 1109–1111.
- [5] D. Volkov and V. Akulov, *Is the Neutrino a Goldstone Particle?*, Phys. Lett. **B46** (1973) 109–110.
- [6] J. Wess and B. Zumino, *A Lagrangian Model Invariant Under Supergauge Transformations*, Phys. Lett. **B49** (1974) 52.
- [7] J. Wess and B. Zumino, *Supergauge Transformations in Four-Dimensions*, Nucl. Phys. **B70** (1974) 39–50.
- [8] S. Weinberg, *Implications of Dynamical Symmetry Breaking*, Phys. Rev. **D13** (1976) 974–996.
- [9] E. Gildener, *Gauge Symmetry Hierarchies*, Phys. Rev. **D14** (1976) 1667.
- [10] S. Weinberg, *Implications of Dynamical Symmetry Breaking: An Addendum*, Phys. Rev. **D19** (1979) 1277–1280.
- [11] L. Susskind, *Dynamics of Spontaneous Symmetry Breaking in the Weinberg- Salam Theory*, Phys. Rev. **D20** (1979) 2619–2625.

[12] C. Giunti, C. W. Kim, and U. Lee, *Running coupling constants and grand unification models*, Mod. Phys. Lett. **A6** (1991) 1745–1755.

[13] J. Ellis, S. Kelley, and D. Nanopoulos, *Probing the desert using gauge coupling unification*, Phys. Lett. **B260** (1991) 131–137.

[14] U. Amaldi, W. de Boer, and H. Furstenau, *Comparison of grand unified theories with electroweak and strong coupling constants measured at LEP*, Phys. Lett. **B260** (1991) 447–455.

[15] P. Langacker and M.-X. Luo, *Implications of precision electroweak experiments for $M(t)$, $\rho(0)$, $\sin^2\Theta(W)$ and grand unification*, Phys. Rev. **D44** (1991) 817–822.

[16] P. Fayet, *Spontaneously Broken Supersymmetric Theories of Weak, Electromagnetic and Strong Interactions*, Phys. Lett. **B69** (1977) 489.

[17] G. R. Farrar and P. Fayet, *Phenomenology of the Production, Decay, and Detection of New Hadronic States Associated with Supersymmetry*, Phys. Lett. **B76** (1978) 575–579.

[18] W. Beenakker, R. Hopker, T. Plehn, and P. Zerwas, *Stop decays in SUSY QCD*, Z. Phys. **C75** (1997) 349–356.

[19] J. Hisano, K. Kawagoe, and M. M. Nojiri, *Detailed study of gluino decay into third generation squarks at the CERN LHC*, Phys. Rev. **D68** (2003) 035007.

[20] C. Balázs, M. Carena, and C. E. M. Wagner, *Dark matter, light top squarks, and electroweak baryogenesis*, Phys. Rev. **D70** (2004) 015007.

[21] M. Mühlleitner, A. Djouadi, and Y. Mambrini, *SDECAY: a Fortran code for the decays of the supersymmetric particles in the MSSM*, Computer Physics Communications **168** (2005) no. 1, 46 – 70. <http://www.sciencedirect.com/science/article/pii/S0010465505000822>.

[22] S. Kraml and A. R. Raklev, *Same-sign top quarks as signature of light stops at the CERN LHC*, Phys. Rev. **D73** (2006) 075002.

[23] ATLAS Collaboration, *Search for supersymmetric particles in events with lepton pairs and large missing transverse momentum in $\sqrt{s} = 7$ TeV proton-proton collisions with the ATLAS experiment*, Eur. Phys. J. **C71**, 1682 (2011).

[24] ATLAS Collaboration, *Searches for supersymmetry with the ATLAS detector using final states with two leptons and missing transverse momentum in $\sqrt{s} = 7$ TeV proton-proton collisions*, arXiv:1110.6189 [hep-ex] (2011).

[25] ATLAS Collaboration, *Search for supersymmetry in pp collisions at $\sqrt{s} = 7$ TeV in final states with missing transverse momentum, b-jets and one lepton with the ATLAS detector*, ATLAS-CONF-2011-130, 2011.

[26] ATLAS Collaboration, *Search for superSymmetry in pp Collisions at $\sqrt{s} = 7$ TeV in final states with missing transverse momentum and b-jets with the ATLAS detector*, To be published.

[27] ATLAS Collaboration, *The ATLAS Experiment at the CERN Large Hadron Collider*, JINST **3** (2008) S08003.

[28] The azimuthal angle ϕ is measured around the beam axis and the polar angle θ is the angle from the beam axis where the pseudorapidity is defined as $\eta = -\ln \tan(\theta/2)$.

[29] ATLAS Collaboration, *Luminosity Determination in pp Collisions at $\sqrt{s}=7$ TeV using the ATLAS Detector at the LHC*, Eur. Phys. J. **C71** (2011) 1630.

[30] ATLAS Collaboration, *Luminosity Determination in pp Collisions at $\sqrt{s} = 7$ TeV using the ATLAS Detector in 2011*, ATLAS-CONF-2011-116, 2011.

[31] M. Cacciari, G. P. Salam, and G. Soyez, *The Anti- $k(t)$ jet clustering algorithm*, JHEP **0804** (2008) 063, arXiv:0802.1189 [hep-ph].

[32] M. Cacciari and G. Salam, *Dispelling the N^3 myth for the k_t jet-finder*, Phys. Lett. B **641** (2006) no. 1, 57 – 61.

[33] ATLAS Collaboration, *Jet energy measurement with the ATLAS detector in proton-proton collisions at $\sqrt{s} = 7$ TeV*, arXiv:1112.6426 [hep-ex] (2011).

[34] ATLAS Collaboration, *Electron performance measurements with the ATLAS detector using the 2010 LHC proton-proton collision data*, arXiv:1110.3174 [hep-ex] (2011).

[35] ATLAS Collaboration, *Muon reconstruction efficiency in reprocessed 2010 LHC proton-proton collision data recorded with the ATLAS detector*, ATLAS-CONF-2011-063, 2011.

[36] ATLAS Collaboration, *Performance of Missing Transverse Momentum Reconstruction in Proton-Proton Collisions at 7 TeV with ATLAS*, Eur. Phys. J. C **72** (2012) 1844.

[37] ATLAS Collaboration, *Search for supersymmetry in final states with jets, missing transverse momentum and one isolated lepton in $\sqrt{s} = 7$ TeV pp collisions using 1 fb^{-1} of ATLAS data*, Phys. Rev. **D85** (2012) 012006.

[38] ATLAS Collaboration, *Performance of primary vertex reconstruction in proton-proton collisions at $\sqrt{s} = 7$ TeV in the ATLAS experiment*, ATLAS-CONF-2010-069, 2010.

[39] A. H. Chamseddine, R. L. Arnowitt and P. Nath, Phys. Rev. Lett. **49** (1982) 970; R. Barbieri, S. Ferrara and C.A. Savoy, Phys. Lett. **B119** (1982) 343; L.E. Ibanez, Phys. Lett. **B118** (1982) 73; L.J. Hall, J.D. Lykken and S. Weinberg, Phys. Rev. **D27** (1983) 2359; N. Ohta, Prog. Theor. Phys. **70** (1983) 542, 1982.

[40] Kane, G. and Kolda, C. and Roszkowski, L. and Wells, J., *Study of constrained minimal supersymmetry*, Phys. Rev. **D49** (1994) 6173–6210.

[41] S. Frixione and B. Webber, *The MC@NLO 3.2 Event Generator*, arXiv:hep-ph/0601192 (2006).

[42] P. Nadolsky *et al.*, *Implications of CTEQ global analysis for collider observables*, Phys. Rev. **D78** (2008) 013004.

[43] M. Mangano *et al.*, *ALPGEN, a generator for hard multiparton processes in hadronic collisions*, JHEP **07** (2003) 001.

[44] J. Pumplin *et al.*, *New generation of parton distributions with uncertainties from global QCD analysis*, JHEP **07** (2002) 012.

[45] G. Corcella *et al.*, *HERWIG 6: An event generator for hadron emission reactions with interfering gluons (including supersymmetric processes)*, JHEP **01** (2001) 010.

[46] J. Butterworth, J. R. Forshaw, and M. Seymour, *Multiparton interactions in photoproduction at HERA*, Z. Phys. **C72** (1996) 637–646.

[47] J. Alwall, M. Herquet, F. Maltoni, O. Mattelaer, and T. Stelzer, *MadGraph 5 : Going Beyond*, JHEP **06** (2011) 128.

[48] T. Sjöstrand, S. Mrenna, and P. Skands, *PYTHIA 6.4 Physics and Manual*, JHEP **0605** (2006) 026.

[49] A. Lazopoulos, T. McElmurry, K. Melnikov, and F. Petriello, *Next-to-leading order QCD corrections to $t\bar{t}Z$ production at the LHC*, Phys. Lett. **B666** (2008) 62–65.

[50] Frank Petriello, private communication, 2011.

[51] W. Beenakker, M. Kramer, T. Plehn, M. Spira, and P. Zerwas, *Stop production at hadron colliders*, Nucl. Phys. **B515** (1998) 3–14.

[52] D. Stump *et al.*, *Inclusive jet production, parton distributions, and the search for new physics*, JHEP **10** (2003) 046.

[53] ATLAS Collaboration, *First tuning of HERWIG/JIMMY to ATLAS data*, ATL-PHYS-PUB-2010-014, 2010 and *Charged particle multiplicities in $p p$ interactions at $\sqrt{s} = 0.9$ and 7 TeV in a diffractive limited phase-space measured with the ATLAS detector at the LHC and new PYTHIA6 tune*, ATLAS-CONF-2010-031, 2010.

[54] ATLAS Collaboration, *The ATLAS Simulation Infrastructure*, Eur. Phys. J. **C70** (2010) 823–874.

[55] S. Agostinelli *et al.*, *GEANT4: A simulation toolkit*, Nucl. Instrum. Meth. **A506** (2003) 250–303.

[56] ATLAS Collaboration, *Measurement of the top quark-pair production cross section with ATLAS in $p p$ collisions at $\sqrt{s} = 7$ TeV*, Eur. Phys. J. **C71** (2011) 1577.

[57] ATLAS Collaboration, *Measurement of the top quark pair production cross section in $p p$ collisions at $\sqrt{s} = 7$ TeV in dilepton final states with ATLAS*, Phys. Lett. **B707** (2012) 459–477.

[58] A. L. Read, *Presentation of search results: The $CL(s)$ technique*, J. Phys. G **G28** (2002) 2693–2704.

[59] F. E. Paige, S. D. Protopopescu, H. Baer, and X. Tata, *ISAJET 7.69: A Monte Carlo event generator for $p p$, anti- p p , and $e+e-$ reactions*, arXiv:0312045 [hep-ph] (2003).

[60] T. Aaltonen *et al.* (CDF Collaboration), *Inclusive Search for Squark and Gluino Production in $p\bar{p}$ Collisions at $\sqrt{s} = 1.96$ -TeV*, Phys. Rev. Lett. **102** (2009) 121801.

[61] V. M. Abazov, *et al.* (D0 Collaboration), *Search for squarks and gluinos in events with jets and missing transverse energy using 2.1 fb^{-1} of $p\bar{p}$ collision data at $\sqrt{s} = 1.96$ TeV*, Phys. Lett. **B660** (2008) 449–457.

[62] V. M. Abazov, *et al.* (D0 Collaboration), *Search for scalar bottom quarks and third-generation leptoquarks in $p\bar{p}$ collisions at $\sqrt{s} = 1.96$ TeV*, Phys. Lett. **B693** (2010) 95–101.

[63] LEP SUSY Working Group (ALEPH, DELPHI, L3, OPAL), Notes LEPSUSYWG/01-03.1 and 04-02.1, <http://lepsusy.web.cern.ch/lepsusy/Welcome.html>.

[64] ATLAS Collaboration, *Search for new phenomena in final states with large jet multiplicities and missing transverse momentum using $\sqrt{s}=7$ TeV $p p$ collisions with the ATLAS detector*, JHEP **1111** (2011) 099.

[65] ATLAS Collaboration, *Search for squarks and gluinos using final states with jets and missing transverse momentum with the ATLAS detector in $\sqrt{s} = 7$ TeV proton-proton collisions*, arXiv:1110.2299 [hep-ex] (2011).